

Characterization of novel *CYP2C8* haplotypes and their contribution to paclitaxel and repaglinide metabolism

Running title: *CYP2C8* haplotypes and altered drug metabolism

Cristina Rodríguez-Antona^{a,b}, Mikko Niemi^c, Janne T. Backman^c, Lauri I. Kajosaari^c, Pertti J. Neuvonen^c, Mercedes Robledo^b and Magnus Ingelman-Sundberg^a

^a Section of Pharmacogenetics, Department of Physiology and Pharmacology, Karolinska Institute, Stockholm, Sweden

^b Hereditary Endocrine Cancer Group, Human Cancer Genetics Programme, Spanish National Cancer Center (CNIO), Madrid, Spain

^c Department of Clinical Pharmacology, University of Helsinki and Helsinki University Central Hospital, Helsinki, Finland

Corresponding author address:

Dr. Cristina Rodríguez-Antona,
Hereditary Endocrine Cancer Group
Human Cancer Genetics Programme
Spanish National Cancer Center (CNIO)
Melchor Fernández Almagro 3
28029 Madrid, Spain
Tel. +34 912246948; Fax. +34 912246923
E-mail: cristina.rodriguez-antona@cnio.es

ABSTRACT

Cytochrome P450 2C8 (CYP2C8) plays a major role in the metabolism of therapeutically important drugs which exhibit large interindividual differences in their pharmacokinetics. In order to evaluate any genetic influence on this variation a *CYP2C8* phenotype-genotype evaluation was carried out in Caucasians. Two novel *CYP2C8* haplotypes, named B and C with frequencies of 24 and 22% in Caucasians, respectively, were identified and caused a significantly increased and reduced paclitaxel 6 α -hydroxylation, respectively, as evident from analyses of 49 human liver samples. In healthy white subjects, *CYP2C8**3 and the two novel haplotypes significantly influenced repaglinide pharmacokinetics in *SLCO1B1*c.521 heterozygous individuals: haplotype B was associated with reduced and haplotype C with increased repaglinide AUC (0- ∞). Functional studies suggested -271C>A (*CYP2C8**1B) as a causative SNP in haplotype B. In conclusion, two novel common *CYP2C8* haplotypes were identified and significantly associated with altered rate of CYP2C8 dependent drug metabolism *in vitro* and *in vivo*.

Keywords: Cytochrome P450 2C8 (CYP2C8), haplotype, SNP, paclitaxel, repaglinide, pharmacogenetics.

Abbreviations: AUC(0- ∞), area under the plasma concentration-time curve from time 0 to infinity; CYP, cytochrome P450; HPLC, high performance liquid chromatography; PCR, polymerase chain reaction; SNP, single nucleotide polymorphism.

INTRODUCTION

Cytochrome P450 2C8 (CYP2C8) is a drug-metabolizing enzyme mainly expressed in the liver but also present in the gastrointestinal tract, kidney, adrenal gland and tonsils¹. CYP2C8 plays a major role in the metabolism of several clinically important therapeutic drugs such as amiodarone, amodiaquine, dapsone, loperamide, paclitaxel, pioglitazone, repaglinide, rosiglitazone, and verapamil²⁻⁵. In addition, CYP2C8 oxidizes the endogenous substrate arachidonic acid to vasoactive epoxyeicosatrienoic acids and it has been proposed that CYP2C8 might be relevant for cardiovascular disease processes^{6, 7}. There is a large interindividual variation in the metabolism of CYP2C8-specific substrates and in CYP2C8 expression⁸, which is likely to influence the therapeutic or adverse outcome of drugs metabolized by CYP2C8. For example, CYP2C8 is a key enzyme in the metabolic pathway of cerivastatin^{9, 10}, which was withdrawn from the market in 2001 because of a high risk of myotoxicity. Gemfibrozil, a potent inhibitor and inactivator of CYP2C8 greatly increased the plasma concentrations of cerivastatin and the risk of rhabdomyolysis¹¹. Clinically relevant interindividual differences in CYP2C8 activity might be the result of *CYP2C8* gene polymorphisms. To date, several CYP2C8 variant proteins caused by single nucleotide polymorphisms (SNPs) have been described (see <http://www.cypalleles.ki.se>) although no common deleterious allelic variant has been identified^{10, 12-14}.

Paclitaxel 6 α -hydroxylation is commonly used as a marker reaction for CYP2C8 activity *in vitro*. Paclitaxel is metabolized by P450s in the liver, mainly by CYP2C8 (6 α -hydroxylation) and also by CYP3A4 (C'3-hydroxylation)¹⁵. Several lines of evidence are in support of CYP2C8 being the major catalyst of 6 α -hydroxylation of paclitaxel, such as the correlation between the formation of 6 α -OH-paclitaxel and the hepatic CYP2C8 protein content and in addition the

formation of other metabolites formed by CYP2C8^{16,17}. Furthermore, the selective and potent *in vitro* CYP2C8-inhibitor montelukast which inhibits several CYP2C8-specific reactions such as amodiaquine N-deethylase, rosiglitazone N-demethylase, also effectively inhibits paclitaxel 6 α -hydroxylase¹⁸.

In the present study, we conducted a systematic investigation about *CYP2C8* genetic variation and its impact on CYP2C8 phenotype. Using data from the International HapMap Project and direct genotyping of 54-unrelated human samples, the common *CYP2C8* Caucasian haplotypes were inferred. The data was used to perform haplotype-phenotype association studies using a human liver panel in which CYP2C8 activity and expression levels were characterized and repaglinide pharmacokinetics data obtained from white healthy volunteers. Two novel *CYP2C8* haplotypes (named B and C) which might explain part of the interindividual differences in CYP2C8 activity were found.

RESULTS

CYP2C8 interindividual variation affects hepatic CYP2C8 mRNA and protein content and *in vitro* paclitaxel 6 α -hydroxylation

To identify major factors contributing to CYP2C8 interindividual variation we used a human liver panel (n=54). The activity of CYP2C8 was determined by measuring the CYP2C8-specific paclitaxel 6 α -hydroxylation. The CYP2C8 inter-sample variation was 190 and 23-fold at the level of mRNA and protein content, respectively, and 34-fold at the level of activity. A correlation between CYP2C8 mRNA and protein content was found, suggesting that the variable CYP2C8 protein expression levels could be controlled by a pre-translational mechanism. Similarly, the CYP2C8 protein content essentially paralleled the rate of paclitaxel 6 α -hydroxylation (Figures 1 A and B).

Neither gender nor age influenced *CYP2C8* expression (data not shown). Interestingly, an alternatively spliced CYP2C8 mRNA carrying the full sequence of intron 2 was detected by RT-PCR (data not shown). The relative levels of the splicing products were however similar in all samples (data not shown), suggesting that the alternative splicing is not the cause for the inter-individual CYP2C8 variation.

Identification of the common Caucasian *CYP2C8* haplotypes

Using the HapMap Project CEPH data we found that the *CYP2C8* gene was included in one single haplotype block in Caucasians (Supplementary Figure 1A) and that *CYP2C8* diversity was captured by 7 common haplotypes (frequency > 2%). Twelve *CYP2C8* SNPs (HapMap tagging SNPs and *CYP2C8* SNPs with a putative functional role: located in coding regions, proximal promoter and near splicing sites) were selected and genotyped by allele specific PCR or RFLP in

54 unrelated Caucasian liver samples, *CYP2C8* haplotypes were inferred and then compared to HapMap data. The results were very similar to HapMap, and 7 common *CYP2C8* haplotypes were also identified and named: A, B, C1, C2, C3, D and E (Table 1). The major difference between HapMap and the haplotypes predicted with the liver samples consisted in HapMap haplotype F which was almost absent in the livers (0.4% frequency) and *CYP2C8*4* (not present in HapMap database) which differentiated haplotypes C1 and C2. Asians and Africans showed important variations in the *CYP2C8* haplotype blocks, haplotypes and in the frequency of *CYP2C8* SNPs, for example, haplotype D (*CYP2C8*3*) was only detected in Caucasians (Supplementary Figure 2).

Two *CYP2C8* haplotypes show an altered phenotype *in vitro* and *in vivo*

Livers carrying the variant alleles, *CYP2C8*3* and *CYP2C8*4* causing amino acid substitutions, did not show a significantly altered paclitaxel 6 α -hydroxylation in comparison to *CYP2C8*1/*1* livers. There were 13 *CYP2C8*3* and 8 *CYP2C8*4* heterozygous from a total of 49 liver samples and the mean activity after excluding from the analysis one sample carrying simultaneously *3 and *4 alleles was: 39.8, 30.2 and 31.8 6 α -hydroxypaclitaxel ng/min/mg protein, for *CYP2C8*1/*1*, *CYP2C8*1/*3* and *CYP2C8*1/*4* samples, respectively, with no significant differences. These results suggest that these variants do not have a large impact on their on a large impact on paclitaxel 6 α hydroxylation, but further studies including homozygous samples and larger numbers should clarify this.

We then compared the *CYP2C8* activity (measured by paclitaxel 6 α -hydroxylation) and the *CYP2C8* haplotypes of the liver samples (n = 49), and found that neither haplotypes A, D, nor E showed a significantly different activity (data not shown). On the other hand, haplotype B was

associated with an increased paclitaxel metabolism and haplotype C (grouping together C1, C2, and C3) with a lower activity. When the liver samples carrying *CYP2C8* haplotypes B and C (cases simultaneously carrying both haplotypes excluded from these groups) were compared to the other samples, a statistically significant difference was found for *CYP2C8* activity and protein content (Figure 2). None of the three C haplotypes C1, C2, and C3, when analyzed individually, showed any significant difference in paclitaxel hydroxylation activity. These data highlight *CYP2C8* haplotypes B and C as possible factors contributing to *CYP2C8* inter-individual variability, and suggest that alterations at the enzyme expression level rather than alterations of the enzyme activity could cause the observed differences.

To further evaluate the significance of the *in vitro* *CYP2C8* haplotype-phenotype findings we carried out an analysis of repaglinide pharmacokinetics in 68 white healthy volunteers in relation to the *CYP2C8* haplotypes (Figure 3 and Supplementary Figure 3). Because the coding SNP 521T>C in the *SLCO1B1* gene (Val174Ala; OATP1B1) influences the pharmacokinetics of repaglinide to a large extent, the data were stratified for this SNP. In subjects heterozygous for *SLCO1B1*c.521T/C (with intermediate repaglinide AUC (0-∞) values) the carriers of *CYP2C8* haplotype B or *CYP2C8**3 (haplotype D) had a significantly lower mean AUC (0-∞) of repaglinide (34% and 50% reduction, $P=0.036$ and $P=0.035$, respectively) than non-carriers, whereas haplotype C carriers had a significantly increased mean AUC (0-∞) (34% increase, $P=0.046$) compared to non-carriers (Figure 3). Furthermore, the two *SLCO1B1* 521TC subjects simultaneously carrying haplotypes B and D were those with the lowest repaglinide AUC(0-∞) values (66% lower mean AUC(0-∞) , $P=0.019$). The comparison in subjects homozygous for *SLCO1B1*c.521T/T in general did not reach statistical significance, although, when we compared the repaglinide AUC of the individuals carrying 2 high activity haplotypes (B/B, D/D and B/D,

with 2, 0 and 5 individuals in each group, respectively) with the rest of individuals, a 35% reduced mean AUC(0-∞) of repaglinide ($P=0.05$) was found for the high activity homozygous group (Supplementary Figure 3). The number of individuals with the *SLCO1B1* 521CC genotype was insufficient to perform statistical analysis with respect to *CYP2C8* haplotypes.

***CYP2C8*1B* is a causal SNP in haplotype B**

Despite the high sequence similarity between haplotypes B and E, only haplotype B showed an altered *CYP2C8* activity. Because the results presented above suggest that the rate of transcription might be causative for the interindividual differences in *CYP2C8* expression, we focused on haplotype B promoter SNPs: rs7909236 (*CYP2C8*1B*) and rs11188172, located at -271 and -2048 from the translational start, respectively. Electrophoretic mobility shift assays (EMSAs) showed that a high-affinity protein-DNA specific complex was formed using the *CYP2C8*1B* probe and that the nuclear proteins had higher affinity for the *CYP2C8*1B* element as compared to the wild type *CYP2C8*I* sequence (Figure 4A). The -2048 SNP was located in an element similar to a CAR/PXR site (-2056). However, previous work showed that this site is not functional and can not bind CAR or PXR¹⁹. Similarly, when we performed EMSA experiments with probes containing rs11188172 at -2048, no specific binding complex could be detected neither for the wild type and the variant allele (data not shown).

To further investigate *CYP2C8*1B* functionality, we cloned the -361/-1 *CYP2C8* promoter region corresponding to *CYP2C8*I* (-271C) and *CYP2C8*1B* (-271A) into luciferase reporter plasmids. Transfection of these constructs in the hepatic cell line HepG2 resulted in no differences in luciferase activity (data not shown). However, these cells hardly express *CYP2C8*, suggesting that HepG2 might lack transcriptional factors crucial for *CYP2C8* transcription. Thus,

we transfected the plasmids into mice liver which contains high levels of hepatic transcription factors. As shown in Figure 4B, *CYP2C8*1B* was able to drive transcription at higher rates than *CYP2C8*1* (1.8-fold increase, $P<0.05$). Together all these data suggest that *CYP2C8* -271C>A is a functional polymorphism causing increased activity of haplotype B.

DISCUSSION

This study compared *CYP2C8* genetic variation with *in vitro* and *in vivo* *CYP2C8* phenotype data, in order to elucidate the basis for the inter-individual variation in *CYP2C8* activity. We inferred the common Caucasian *CYP2C8* haplotypes and found that two of them (named B and C) showed an altered *in vitro* paclitaxel metabolism using human liver samples. This effect was also found *in vivo* with repaglinide in *SLCO1B1* 521T/C heterozygous individuals: repaglinide AUC (0-∞) was significantly lower for haplotype B carriers and significantly higher for haplotype C carriers, corresponding to the paclitaxel 6 α -hydroxylation rates in the liver samples (compare Figures 2 and 3). In addition, in the *SLCO1B1* 521T/C heterozygous subjects we also found that haplotype D (*CYP2C8**3) showed a significantly decreased repaglinide AUC (0-∞). However, for the *SLCO1B1* 521T/T homozygous healthy volunteers (with the highest hepatic repaglinide up-take), the effect of the *CYP2C8* haplotypes and *CYP2C8**3 could not be observed, possibly because of the greater impact of CYP3A4 on repaglinide metabolism at higher drug concentrations⁴. Nevertheless, the repaglinide AUC(0-∞) of individuals carrying simultaneously two high activity haplotypes (B and/ or D) was lower than that of individuals carrying none or only 1 or none of these alleles ($P=0.05$).

The impact of *CYP2C8**3 on drug metabolism is still ambiguous. Our study confirms previous pharmacokinetic data showing an increased activity for *CYP2C8**3²⁰⁻²², but this is in contrast to the lack of effect or decreased activity found for *CYP2C8**3 in *in vitro* studies using human liver microsomes or recombinant *CYP2C8.3* protein^{8, 13, 16, 23, 24}. A number of explanations have been proposed for these contradictions, such as differences in *CYP2C8.3* enzymatic activity depending on the substrate, since a variety of substrates have been used, or studies with small sample sizes. Our *in vitro* work using paclitaxel fails to find any effect of

*CYP2C8*3*. However, in a sample set with many *CYP2C8*3* homozygous a relationship might have been evident. In contrast, the *CYP2C8* haplotypes B and C exhibited the same effect *in vitro* with paclitaxel and *in vivo* with repaglinide. Despite that the allele frequency of the two novel *CYP2C8* haplotypes, B and C, was relatively high (24 and 22%, respectively, calculated with the 122 Caucasian samples included in the study), the number of subjects homozygous for haplotype B and C was low in our study resulting in an underpowering effect of the haplotypes and hence rendering it difficult to calculate the difference in *CYP2C8* drug metabolism for these individuals. Thus, further studies are needed to fully evaluate the clinical impact of the novel *CYP2C8* haplotypes, as well as *CYP2C8*3*, on *CYP2C8* dependent drug-metabolism.

In addition, we tried to find the functional SNPs within the *CYP2C8* haplotypes. Since there is one single haplotype block within the *CYP2C8* gene in Caucasians, all SNPs are in linkage disequilibrium and the causative SNPs could be located anywhere within the gene (Supplementary Figure 1). However, we focused on haplotype B-specific promoter SNPs because previous data suggested that mRNA levels are important for *CYP2C8* inter-individual variation. We tested these SNPs using EMSA analysis and plasmid mice transfection, and found that *CYP2C8*1B* affected both transcription factor binding and promoter activity (Figure 4), thus, suggesting that this is a causative SNP within haplotype B. With respect to inter-ethnic differences, in Asians and Africans there are 2 and 3 haplotype blocks within *CYP2C8* gene, respectively, and the frequency of some *CYP2C8* SNPs is very different from Caucasians: *CYP2C8*3* (Haplotype D) is absent in Asians and Africans and *CYP2C8*1B* is also found in Asians but is not associated to any specific haplotype because its location in a recombination region (supplementary Figure 2).

An optimized therapy for drugs metabolized by *CYP2C8* might require the identification of individuals with higher risk of adverse drug reactions, due to a reduced rate of metabolism, and

of those which might need higher drug doses, due to an increased metabolism. This is particularly warrant for drugs with narrow therapeutic indexes that frequently present serious toxicities such as the anti-cancer drug paclitaxel. In this respect, the genetic variation of *CYP2C8* could play an important role and this work provides novel data regarding the relevant polymorphism involved.

In conclusion, the *CYP2C8* phenotype shows a large interindividual variability that, to a certain extent, is due to genetic variations predictable by genotyping. The two novel Caucasian *CYP2C8* haplotypes identified in this work (named B and C and characterized by rs7909236 (*CYP2C8*1B*) and rs1113129/rs3216029, respectively: Figure 5) might contribute to a better dose optimization by predictive genotyping in patients on therapy with drugs which are *CYP2C8* substrates.

MATERIALS AND METHODS

Materials

Protease Inhibitor Cocktail Tablets were from Roche Diagnostics (Mannheim, Germany). Paclitaxel was from Sigma (St Louis, MO) and 6 α -hydroxy paclitaxel was from BD Gentest (Woburn, Mass). [γ -³²P]dATP was purchased from Amersham Biosciences (Freiburg, Germany). Poly(dIdC) was purchased from Pharmacia (Peapack, NJ). The Dual Luciferase Reporter Assay System, the pGL3-Basic firefly luciferase reporter vector and the pRL-SV40 Renilla plasmid were from Promega (Madison, WI). The TransIT[®] In vivo Gene Delivery System kit was from Mirus (Madison, WI).

Human Liver Material

The characteristics of the 54 livers used in this have been previously described^{25, 26}. All livers were documented to be of Caucasian origin except for one of unknown origin, which showed typical Caucasian haplotype characteristics and was included in the study. The tissues were stored at -70°C until used to isolate total RNA, genomic DNA, and to prepare microsomes by subcellular fractionation.

Drug pretreatment data from the liver donors showed that in 7 cases they had previously taken some CYP3A inducers, which could plausibly affect CYP2C8 levels. We compared the CYP3A4 (previously described)^{25, 26} and CYP2C8 activities of the liver samples finding a correlation coefficient of 0.35 and r^2 of 0.13. The CYP2C8 mRNA, protein and activity levels of the livers with no drug induction and of those putatively induced was compared finding in average a 0.8, 1.6 and 1.0-fold difference in the induced livers when compared with the non-treated livers (for

CYP3A4 the induced livers showed a 2.5-fold increase in activity). This suggested that for CYP2C8, the possible induction in those 7 livers, was not a major confounding factor in the study.

RT-PCR for CYP2C8 mRNA quantification and detection of CYP2C8 alternative splicing

Total RNA was extracted from the human livers using the QuickPrepTotal RNA Extraction Kit (Amersham Biosciences) and 2 µg of total RNA were reverse transcribed using Super-script II Reverse Transcriptase (Invitrogen) and an oligo dT14 primer. The cDNAs from the human livers were subjected to standard PCR amplification using specific primers. Quantitative real-time PCR assay was carried out with the Smart Cycler (Cepheid) using the SyberGreen PCR master mix (PE Applied Biosystems) and primers specifically amplifying the correctly spliced or the alternatively spliced CYP2C8 mRNA and β-actin (Supplementary Table 1). Aliquots of the PCR reactions were subjected to electrophoresis, for size and purity confirmation. Standard curves were constructed with serial 10-fold dilutions of an accurately determined concentration of a DNA fragment containing the target sequence. Normalization was carried out with the internal standard β-actin.

Immunoblot analysis

Quantification of CYP2C8 protein in human liver microsomes was performed by immunoblotting analysis using the anti human CYP2C8 antibody from Puracyp (Carlsbad, CA) which does not cross-react with CYP2C9, CYP2C18 or CYP2C19. Basically, Western blotting was performed as previously described and following the antibody manufacturer's instructions ²⁷. The CYP2C8 content was determined from standard curves derived from human CYP2C8 BD Supersomes (BD

Gentest). The detection limit under the conditions used was of 2.5 pmol CYP2C8/ mg microsomal protein.

Assay for paclitaxel 6 α -hydroxylase activity

Paclitaxel 6 α -hydroxylase activity was determined as described previously²³ with slight modifications. The incubation mixture contained 10 μ M paclitaxel, 300 μ g of microsomal proteins and 1 mM NADPH in a final volume of 0.5 ml of 50 mM potassium phosphate buffer (pH 7.4). After preincubation for 1 min at 37 °C, the reaction was started by the addition of NADPH. The mixture was incubated for 40 min at 37 °C, and the reaction was stopped with 3 ml of ethyl acetate. The mixture was spiked with internal standard (4-androstene 3,17-dione) and vigorously vortexed for 5 min. After centrifugation at 5,000 g for 10 min, the organic fraction was evaporated under a gentle stream of N₂ gas. High-performance liquid chromatography (HPLC) analysis was performed injecting the samples into a 5 μ m 4 x 250 mm LiChrospher-100 RP-18 column (Merck, Darmstadt, Germany) using a 60:40 methanol:H₂O (v/v) isocratic mobile phase at a flow rate of 1 ml/ min and peaks detected by UV absorbance at 229 nm. Quantification of 6 α -hydroxy paclitaxel was based on peak area measurements from linear calibration curves obtained with pure reference compounds. The detection limit was 2.5 ng 6 α -hydroxy paclitaxel min⁻¹ mg prot⁻¹. Samples incubated without NADPH were used to determine background absorbance. The results presented are the mean of independent microsomal incubations, except for 10 samples where only one incubation could be performed.

CYP2C8 genotyping and sequencing

Genomic DNA from the human livers was prepared using a QIAamp tissue kit (QIAGEN GmbH, Hilden, Germany), the final DNA concentration was determined using PicoGreen (Molecular Probes, Leiden, The Netherlands) and 50 ng of DNA were used for each genotyping.

RFLP was used for the genotyping of *CYP2C8*1C*, *CYP2C8*3-R139K*, rs1113129, rs11188172 and rs1934956, while allele specific PCR was used for *CYP2C8*1B*, *CYP2C8*3-K399R*, *CYP2C8*4*, rs2275622, rs3216029, rs2275620 and rs2185571. The oligonucleotides used for *CYP2C8* genotyping, the size of the amplified DNA fragment and, in case of RFLP, the restriction enzymes used are listed in Supplementary Table 2. In general, the amplification conditions for RFLP were: 1 min 95°C, followed by 36 cycles of 30 s at 94°C, 30 s at 57°C, 30-60s at 72°C and a final extension of 5 min at 72°C, using the *Taq* polymerase from Invitrogene. For allele specific PCRs the annealing temperatures and number of cycles varied and are available upon request.

Genotyping accuracy was ascertained through direct sequencing of random homozygous wild type, homozygous variant and heterozygous samples using the ABI PRISM BigDye Terminator Cycle Sequencing Ready Reaction Kit and analyzed on an ABI PRISM 377 DNA Sequencer (Applied Biosystems). No deviations from the expected population genotype proportions (predicted by Hardy-Weinberg Equilibrium) were detected.

***CYP2C8* haplotype inference**

The data from the International HapMap project (<http://www.hapmap.org>) was used to identify *CYP2C8* tagging SNPs (tSNPs) capturing the haplotype diversity of *CYP2C8*. The SNPs genotype data was dumped from the International HapMap Project ²⁸ and analyzed using Haploview 3.32 (<http://www.broad.mit.edu/personal/jcbarret/haplo/download.php>) ²⁹. In

Caucasians *CYP2C8* gene was contained in one haplotype block and 6 tSNPs represented the 7 haplotypes with a frequency higher than 0.02 (Supplementary Figure 1).

In an independent sample series of 54 unrelated Caucasian samples we inferred *CYP2C8* haplotypes by genotyping 12 *CYP2C8* SNPs (HapMap tSNPs which are underlined plus additional putatively important *CYP2C8* SNPs): the coding SNPs *CYP2C8**3 (rs11572080 and rs10509681) and *CYP2C8**4 (rs1058930); the promoter SNPs *CYP2C8**1B (rs7909236), *CYP2C8**1C (rs17110453) and a SNP located in a putative CAR-PXR element at -2048 (rs11188172), two intron 2 SNPs of relatively high frequency IVS2-64G>A (rs2275622) and IVS2-13insT (rs11572078) and SNPs characteristic of different HapMap haplotypes: rs1934956 in intron 1, rs2185571 in intron 3, rs1113129 in intron 5 and rs2275620 in intron 7. In 51 samples the genotype data was complete for the 12 SNPs and SNPalyze 4.1 software (Dynacom Co., Ltd. in Japan) and PHASE program^{30,31} were used for haplotype inference (Table 1).

Repaglinide pharmacokinetics in relation to *CYP2C8* haplotypes in humans *in vivo*

A total of 68 healthy Finnish Caucasian subjects, who had participated in pharmacokinetic studies with repaglinide were included³²⁻³⁷. The studies had been approved by the Ethics Committee for Studies in Healthy Subjects of the Helsinki and Uusimaa Hospital District and the National Agency for Medicines. All subjects had given written informed consent.

After an overnight fast, the subjects ingested a single 0.25-mg dose of repaglinide (one half of a 0.5-mg tablet of Novonorm; NovoNordisk, Bagsværd, Denmark) with 150 mL of water at 9 AM. Repaglinide concentrations were quantified in timed plasma samples for up to 7 hours by liquid chromatography–tandem mass spectrometry. The area under the plasma repaglinide concentration-time curve from time 0 to infinity, AUC(0-∞), was calculated as described previously³²⁻³⁷.

A 10-ml EDTA blood sample was drawn from each subject and stored at -20°C prior to genomic DNA extraction with the QIAamp blood DNA mini kit (Qiagen). Of the 68 subjects, 56 had been genotyped for the *SLCO1B1*c521T>C SNP previously and the remaining 12 were genotyped for that SNP as described previously²¹. In order to assign the corresponding *CYP2C8* haplotypes to the subjects, 6 tSNPs were genotyped: rs7909236 (*CYP2C8**1B= haplotype B); rs1113129 (intron 5= haplotype C=C1+C2+C3); rs17110453 (*CYP2C8**1C= haplotype C1+C2); rs1058930 (*CYP2C8**4= haplotype C2); rs11572080 (*CYP2C8**3= haplotype D); rs2275622 (intron 2-64G>A= haplotype E when rs7909236 is negative) and haplotype A was assigned when negative for the 6 SNPs above.

Preparation of nuclear extracts and electrophoretic mobility shift assay (EMSA)

Nuclear extracts from HepG2 cells were prepared as described previously³⁸. The double stranded oligonucleotides corresponding to *CYP2C8**1 and *CYP2C8**1B were 5'-CAGCACATTGGAACAACCAGGGACT-3' and 5'-CAGCACATTGGAAAAACCAGGGACT-3', respectively, and their inverse/ complementary sequences. The double stranded oligonucleotides corresponding to rs11188172 G>A, at -2048 of *CYP2C8* were 5'- AAACCAAACACGTCTGACCCACAT -3' and 5'- AAACCAAACACATCTGACCCACA-3', respectively, and their inverse/ complementary sequences. The EMSA binding reactions were carried out with twelve micrograms of nuclear extract that were preincubated at 37 °C for 20 min in a buffer containing 2 µg of poly(dI/dC), 100 mM of NaCl, 15 mM HEPES pH 7.9, 0.25 mM EDTA, 0.25 mM EGTA, 0.25 mM dithiothreitol and 5 % glycerol. The oligonucleotides were radiolabeled using [³²P] dATP and T4 polynucleotide kinase (Invitrogen), added to the reaction mixture that had a final volume of 25µl,

and incubated for 30 min at 37 °C. For competition experiments, 5 to 50-fold excess of unlabeled double stranded oligonucleotides were added to the reaction mixture before the radiolabeled probe. The binding of proteins to the oligonucleotides was determined by fractionating the reaction mixture by electrophoresis through a nondenaturing 4% polyacrylamide gel at 200 V and 4 °C, using 0.5 x TBE buffer. Where appropriate, a competitor DNA was included in the preincubation, prior to the addition of the ³²P labeled DNA. Gels were dried and exposed at –70°C to an X-ray film with intensifying screens.

Reporter plasmids and *in vivo* mouse liver cell transfection

Fragments of the human *CYP2C8* promoter were amplified with the Elongase Enzyme Mix (Invitrogen) using genomic DNA from individuals homozygous for the wild type or the *CYP2C8*1B* allele. The primers used were: 5'-GTCACTCGAGCCCAACTGGTCATTAATCTGAGAATAT-3' that contains a XhoI restriction enzyme site underlined, and 5'-AAGGAAGCTTTGAAGCCTTCTCTTCTTATTAAGACAG -3' that contains a HindIII restriction enzyme site underlined. The amplified DNA fragments containing from -368 to -1 of *CYP2C8* promoter (+1 refers to the translation start site) were cloned in the promoterless pGL3-Basic firefly luciferase reporter vector and sequenced to rule out PCR artefacts.

For *in vivo* cell transfection, 20 to 22 g male CD1 mice were transfected through tail injection with 10 µg of the *CYP2C8* constructs and 100 ng of pRL-SV40, in volumes of 2.0 to 2.2 ml in less than 8 s using the TransIT *in vivo* gene delivery system kit as previously described³⁹. Twenty-four hours later, animals were sacrificed and the liver was removed and homogenized to measure firefly and *Renilla* luminescence. Two independent experiments were performed using

two different maxipreps for each construct, and with a total number of at least 15 mice for each construct. The study was approved by the ethics committee for animal experiments at Karolinska Institutet, Stockholm.

Statistical analysis

Data were analyzed using GraphPad InStat version 3.00 for Windows 95, GraphPad Software, San Diego California USA (<http://www.graphpad.com>). The method of Kolmogorov-Smirnov was used to test for normality, and when it indicated normality, parametric tests were used. One-way ANOVA with Tukey-Kramer post test was used for multiple comparisons. Differences were considered significant when *P* values were less than 0.05.

REFERENCES

1. Enayetallah AE, French RA, Thibodeau MS, Grant DF. Distribution of soluble epoxide hydrolase and of cytochrome P450 2C8, 2C9, and 2J2 in human tissues. *J Histochem Cytochem* 2004; **52**: 447-454.
2. Totah RA, Rettie AE. Cytochrome P450 2C8: substrates, inhibitors, pharmacogenetics, and clinical relevance. *Clin Pharmacol Ther* 2005; **77**: 341-52.
3. Jaakkola T, Laitila J, Neuvonen PJ, Backman JT. Pioglitazone is metabolised by CYP2C8 and CYP3A4 in vitro: potential for interactions with CYP2C8 inhibitors. *Basic Clin Pharmacol Toxicol* 2006; **99**: 44-51.
4. Kajosaari LI, Laitila J, Neuvonen PJ, Backman JT. Metabolism of repaglinide by CYP2C8 and CYP3A4 in vitro: effect of fibrates and rifampicin. *Basic Clin Pharmacol Toxicol* 2005; **97**: 249-56.
5. Niemi M, Tornio A, Pasanen MK, Fredrikson H, Neuvonen PJ, Backman JT. Itraconazole, gemfibrozil and their combination markedly raise the plasma concentrations of loperamide. *Eur J Clin Pharmacol* 2006; **62**: 463-72.
6. Lundblad MS, Stark K, Eliasson E, Oliw E, Rane A. Biosynthesis of epoxyeicosatrienoic acids varies between polymorphic CYP2C enzymes. *Biochem Biophys Res Commun* 2005; **327**: 1052-1057.
7. Yasar U, Bennet AM, Eliasson E, Lundgren S, Wiman B, De Faire U, *et al.* Allelic variants of cytochromes P450 2C modify the risk for acute myocardial infarction. *Pharmacogenetics* 2003; **13**: 715-720.
8. Bahadur N, Leathart JB, Mutch E, Steimel-Crespi D, Dunn SA, Gilissen R, *et al.* CYP2C8 polymorphisms in Caucasians and their relationship with paclitaxel 6 α -hydroxylase activity in human liver microsomes. *Biochem Pharmacol.* 2002; **64**: 1579-1589.

9. Wang JS, Neuvonen M, Wen X, Backman JT, Neuvonen PJ. Gemfibrozil inhibits CYP2C8-mediated cerivastatin metabolism in human liver microsomes. *Drug Metab Dispos.* 2002; **30**: 1352-1356.
10. Ishikawa C, Ozaki H, Nakajima T, Ishii T, Kanai S, Anjo S, *et al.* A frameshift variant of CYP2C8 was identified in a patient who suffered from rhabdomyolysis after administration of cerivastatin. *J Hum Genet* 2004; **49**: 582-585.
11. Backman JT, Kyrklund C, Neuvonen M, Neuvonen PJ. Gemfibrozil greatly increases plasma concentrations of cerivastatin. *Clin Pharmacol Ther* 2002; **72**: 685-91.
12. Cavaco I, Stromberg-Norklit J, Kaneko A, Msellem MI, Dahoma M, Ribeiro VL, *et al.* CYP2C8 polymorphism frequencies among malaria patients in Zanzibar. *Eur J Clin Pharmacol* 2005; **61**: 15-18.
13. Soyama A, Saito Y, Komamura K, Ueno K, Kamakura S, Ozawa S, *et al.* Five novel single nucleotide polymorphisms in the CYP2C8 gene, one of which induces a frame-shift. *Drug Metab Pharmacokinet.* 2002; **17**: 374-377.
14. Weise A, Grundler S, Zaumsegel D, Klotzek M, Grondahl B, Forst T, *et al.* Development and evaluation of a rapid and reliable method for cytochrome P450 2C8 genotyping. *Clin Lab* 2004; **50**: 141-148.
15. Rahman A, Korzekwa KR, Grogan J, Gonzalez FJ, Harris JW. Selective biotransformation of taxol to 6 alpha-hydroxytaxol by human cytochrome P450 2C8. *Cancer Res* 1994; **54**: 5543-6.
16. Taniguchi R, Kumai T, Matsumoto N, Watanabe M, Kamio K, Suzuki S, *et al.* Utilization of human liver microsomes to explain individual differences in paclitaxel metabolism by CYP2C8 and CYP3A4. *J Pharmacol Sci* 2005; **97**: 83-90.

17. Ma B, Subramanian R, Schrag ML, Rodrigues AD, Tang C. Cytochrome P450 2C8 (CYP2C8)-mediated hydroxylation of an endothelin ETA receptor antagonist in human liver microsomes. *Drug Metab Dispos* 2004; **32**: 473-8.
18. Walsky RL, Obach RS, Gaman EA, Gleeson JP, Proctor WR. Selective inhibition of human cytochrome P4502C8 by montelukast. *Drug Metab Dispos* 2005; **33**: 413-8.
19. Ferguson SS, Chen Y, LeCluyse EL, Negishi M, Goldstein JA. Human CYP2C8 is transcriptionally regulated by the nuclear receptors constitutive androstane receptor, pregnane X receptor, glucocorticoid receptor, and hepatic nuclear factor 4alpha. *Mol Pharmacol* 2005; **68**: 747-57.
20. Niemi M, Leathart JB, Neuvonen M, Backman JT, Daly AK, Neuvonen PJ. Polymorphism in CYP2C8 is associated with reduced plasma concentrations of repaglinide. *Clin Pharmacol Ther* 2003; **74**: 380-7.
21. Niemi M, Backman JT, Kajosaari LI, Leathart JB, Neuvonen M, Daly AK, *et al.* Polymorphic organic anion transporting polypeptide 1B1 is a major determinant of repaglinide pharmacokinetics. *Clin Pharmacol Ther* 2005; **77**: 468-78.
22. Kirchheiner J, Thomas S, Bauer S, Tomalik-Scharte D, Hering U, Doroshenko O, *et al.* Pharmacokinetics and pharmacodynamics of rosiglitazone in relation to CYP2C8 genotype. *Clin Pharmacol Ther* 2006; **80**: 657-67.
23. Soyama A, Saito Y, Hanioka N, Murayama N, Nakajima O, Katori N, *et al.* Non-synonymous single nucleotide alterations found in the CYP2C8 gene result in reduced in vitro paclitaxel metabolism. *Biol Pharm Bull* 2001; **24**: 1427-30.
24. Dai D, Zeldin DC, Blaisdell JA, Chanas B, Coulter SJ, Ghanayem BI, *et al.* Polymorphisms in human CYP2C8 decrease metabolism of the anticancer drug paclitaxel and arachidonic acid. *Pharmacogenetics* 2001; **11**: 597-607.

25. Westlind A, Lofberg L, Tindberg N, Andersson TB, Ingelman-Sundberg M. Interindividual differences in hepatic expression of CYP3A4: relationship to genetic polymorphism in the 5'-upstream regulatory region. *Biochem Biophys Res Commun* 1999; **259**: 201-5.
26. Westlind-Johnsson A, Malmebo S, Johansson A, Otter C, Andersson TB, Johansson I, *et al.* Comparative analysis of CYP3A expression in human liver suggests only a minor role for CYP3A5 in drug metabolism. *Drug Metab Dispos* 2003; **31**: 755-61.
27. Rodriguez-Antona C, Jande M, Rane A, Ingelman-Sundberg M. Identification and phenotype characterization of two CYP3A haplotypes causing different enzymatic capacity in fetal livers. *Clin Pharmacol Ther* 2005; **77**: 259-70.
28. Consortium TIH. The International HapMap Project. *Nature* 2003; **426**: 789-96.
29. Barrett JC, Fry B, Maller J, Daly MJ. Haploview: analysis and visualization of LD and haplotype maps. *Bioinformatics* 2005; **21**: 263-5.
30. Stephens M, Scheet P. Accounting for decay of linkage disequilibrium in haplotype inference and missing-data imputation. *Am J Hum Genet* 2005; **76**: 449-62.
31. Stephens M, Smith NJ, Donnelly P. A new statistical method for haplotype reconstruction from population data. *Am J Hum Genet* 2001; **68**: 978-89.
32. Niemi M, Backman JT, Neuvonen M, Neuvonen PJ. Effects of gemfibrozil, itraconazole, and their combination on the pharmacokinetics and pharmacodynamics of repaglinide: potentially hazardous interaction between gemfibrozil and repaglinide. *Diabetologia* 2003; **46**: 347-51.
33. Niemi M, Kajosaari LI, Neuvonen M, Backman JT, Neuvonen PJ. The CYP2C8 inhibitor trimethoprim increases the plasma concentrations of repaglinide in healthy subjects. *Br J Clin Pharmacol* 2004; **57**: 441-7.

34. Kajosaari LI, Backman JT, Neuvonen M, Laitila J, Neuvonen PJ. Lack of effect of bezafibrate and fenofibrate on the pharmacokinetics and pharmacodynamics of repaglinide. *Br J Clin Pharmacol* 2004; **58**: 390-6.
35. Kajosaari LI, Niemi M, Neuvonen M, Laitila J, Neuvonen PJ, Backman JT. Cyclosporine markedly raises the plasma concentrations of repaglinide. *Clin Pharmacol Ther* 2005; **78**: 388-99.
36. Kajosaari LI, Niemi M, Backman JT, Neuvonen PJ. Telithromycin, but not montelukast, increases the plasma concentrations and effects of the cytochrome P450 3A4 and 2C8 substrate repaglinide. *Clin Pharmacol Ther* 2006; **79**: 231-42.
37. Kajosaari LI, Jaakkola T, Neuvonen PJ, Backman JT. Pioglitazone, an in vitro inhibitor of CYP2C8 and CYP3A4, does not increase the plasma concentrations of the CYP2C8 and CYP3A4 substrate repaglinide. *Eur J Clin Pharmacol* 2006; **62**: 217-23.
38. Schreiber E, Matthias P, Muller MM, Schaffner W. Rapid detection of octamer binding proteins with 'mini-extracts', prepared from a small number of cells. *Nucleic Acids Res* 1989; **17**: 6419.
39. Pitarque M, Rodriguez-Antona C, Oscarson M, Ingelman-Sundberg M. Transcriptional regulation of the human CYP2A6 gene. *J Pharmacol Exp Ther* 2005; **313**: 814-22.

ACKNOWLEDGEMENTS

This study was supported by grants from The Swedish Research Council, The Swedish Cancer Foundation, Cristina Rodríguez-Antona's Marie Curie Fellowships of the European Community contract numbers QLG5-CT-2002-51733 and MERG-CG-6-2005-014881, the 'Ramon y Cajal' programme from the Spanish Ministry of Education and Science, and the Sigrid Juselius Foundation (Helsinki, Finland).

Table 1. Common *CYP2C8* haplotypes in Caucasians inferred using the genotype data of 54 unrelated individuals.

refSNP	11188172	17110453	7909236	1934956	3216029	2275622	11572080	2185571	1113129	1058930	2275620	10509681	
		<i>2C8*1C</i>	<i>2C8*1B</i>		<i>11572078</i>		<i>2C8*3</i>			<i>2C8*4</i>		<i>2C8*3</i>	
Location ^a	Pr -2048	Pr -370	Pr -271	I1 -712	I2 -13	I2 -64	E3 R139K	I3 -258	I5 -5337	E5 I264M	I7 +49	E8 K399R	Freq (%) ^b
Hapl-A	G	T	C	G	-	G	G	A	C	C	A	A	30.5
Hapl-B	A	T	A	G	-	A	G	G	C	C	T	A	19.6
Hapl-C1	G	G	C	G	T	G	G	G	G	C	A	A	7.4
Hapl-C2	G	G	C	G	T	G	G	G	G	G	A	A	6.5
Hapl-C3	G	T	C	G	T	G	G	G	G	C	A	A	5.4
Hapl-D	G	T	C	G	-	G	A	G	C	C	A	G	15.3
Hapl-E	G	T	C	A	-	A	G	G	C	C	T	A	6.9
<i>Ancestral^c</i>	<i>G</i>	<i>T</i>	<i>n.a.^d</i>	<i>G</i>	<i>n.a.^d</i>	<i>G</i>	<i>G</i>	<i>G</i>	<i>n.a.</i>	<i>C</i>	<i>A</i>	<i>A</i>	

^a The *CYP2C8* genomic DNA sequence (AL359672) was used as reference. The nucleotide changes are the complementary to those shown in the Supplementary Figure 1 because *CYP2C8* gene is in the minus strand (e.g. rs17110453 is a T>G change but HapMap shows this change as A>C; SNP 105).

^b The frequencies of each haplotype are shown, the 7 most common haplotypes accounting for 92% of all predicted haplotypes.

^c The ancestral sequence is that from *Pan Troglodytes*.

^d n.a. (no alignment).

FIGURE LEGENDS

Figure 1. CYP2C8 mRNA and protein content and *in vitro* paclitaxel 6 α -hydroxylation in a panel of human liver samples. The content of CYP2C8 mRNA, protein and activity was quantified in a panel of 54 human livers. Forty two samples had available simultaneously RNA for mRNA quantification and microsomes for protein and activity measurements. CYP2C8 mRNA content was measured by real-time quantitative RT-PCR, CYP2C8 protein content was quantified by immunodetection using a CYP2C8 specific antibody and CYP2C8 activity was determined by measuring the rate of paclitaxel 6 α -hydroxylation. **A**, There was a reasonably good correlation between CYP2C8 mRNA and protein content ($r^2 = 0.38$; $r = 0.62$; $p < 0.001$) **B**, and between CYP2C8 protein content and activity ($r^2 = 0.45$; $r = 0.67$; $p < 0.001$). **C**, A Western blot illustrating the large interindividual variability in human liver CYP2C8 protein content is shown. The amounts of CYP2C8 protein were calculated by interpolation in a standard curve constructed with samples containing different amounts of CYP2C8 and expressed as pmol CYP2C8/ mg microsomal protein. Relative units (r.u.).

Figure 2. Association between CYP2C8 haplotypes and phenotype in a human liver panel.

Liver samples were classified according to their CYP2C8 haplotypes and compared to: **A**, CYP2C8 activity (paclitaxel 6 α -hydroxylation); **B**, CYP2C8 protein content (CYP2C8 pmol/ mg microsomal protein); and **C**, amounts of correctly spliced CYP2C8 mRNA normalized with β -actin content (ru). The horizontal bars show median values for each genotype group. The *P* value for the one-way ANOVA test is shown if <0.05 . In addition, 2-tailed t-test was significant for Hap B vs Hap C at activity and protein level ($P=0.029$ and $P=0.014$, respectively) and for Hap C vs Others at activity and

protein level (P=0.029 and P=0.018, respectively). Subjects homozygous for the *CYP2C8* haplotypes B and C are shown in white.

Figure 3. *CYP2C8* haplotype/ phenotype comparisons in healthy volunteers using repaglinide as probe drug.

Individual AUC(0-∞) values of repaglinide were measured after a single oral dose of 0.25 mg repaglinide in 17 white healthy subjects heterozygous for *SLCO1B1* 521T>C. Subjects were stratified according to the different *CYP2C8* haplotypes: **A**, high activity haplotypes D (*CYP2C8**3) and B and **B**, for the low activity haplotype C. Subjects homozygous for *CYP2C8* haplotypes B, C and D are represented by open circles, in each of the corresponding graphs. The horizontal bars show median values for each genotype group. The groups were compared by a 2-tailed t-test and the P value shown in each graph.

Figure 4. *CYP2C81B results in an increased binding of nuclear proteins and higher transcription rate.**

A, EMSA experiments using double-stranded oligonucleotides expanding the -260/-284 region of *CYP2C8* promoter were performed as described in the Materials and Methods section using nuclear extracts from HepG2 cells. The competition experiments were performed using 5-, 25- or 50-fold excess of cold double stranded oligonucleotides corresponding to -271C (*1) or -271A (*1B) and the DNA labeled probe corresponded either to *CYP2C8**1 (-271C) or *CYP2C8**1B (-271A). Specific protein complex (S), nuclear extracts (NE), free probe (FP). **B**, Transcriptional analysis of the *CYP2C8* proximal promoter by *in vivo* mouse liver transfections. Ten micrograms of *CYP2C8* promoter constructs (-368/-1) and 100 ng of pRL-SV40 were injected into the tail vein of male CD1 mice.

Twenty-four hours later, animals were sacrificed, and the liver homogenized and used to measure firefly and *Renilla* luminescence. The values given represent luminescence normalized mean values \pm S.D., the number between parentheses indicates the number of mice used with each construct. Statistical differences were evaluated using 2-tailed t-test. Relative units (r.u.).

Figure 5. Schematic representation of *CYP2C8* haplotypes A, B and C. *CYP2C8* gene is represented by a rectangle with the exons in black, the arrows indicate the location of SNPs representative of the haplotypes, the nucleotide change shown below. Haplotype B includes the promoter SNPs: -2014 (rs11188172) and -271 (*CYP2C8*1B*, rs7909236). Haplotype B also contains rs2275622 in intron 2 and rs2275620 in intron 7, but these are not haplotype B specific SNPs, since they are also present in haplotype E. Haplotype C includes SNPs in: *CYP2C8* promoter -370 (rs17110453, *2C8*1C*), intron 2 (rs3216029) and intron 5 (rs1113129), and exon 5 (*2C8*4*, rs1058930). In the case of haplotype C two SNPs (*CYP2C8*1C* and *CYP2C8*4*) are not present in all individuals and the estimated frequencies of these SNPs are shown within brackets.

SUPPLEMENTARY INFORMATION

Supplementary Figure 1. Caucasian *CYP2C8* haplotypes inferred using HapMap data.

A, Linkage disequilibrium plot obtained using Haploview with the HapMap CEPH data (European ancestry) from the chromosome10 (positions 96782845 to 96822844) which contains *CYP2C8* gene (minus strand) plus 3.6 kb of the promoter and 3'UTR. Because *CYP2C8* is located in the minus strand, the nucleotide changes shown by HapMap are complementary to those described for *CYP2C8* (e.g. SNP n° 105: rs17110453 which corresponds to *CYP2C8***IC* -370T>G is shown as A>C). Bright red squares correspond to $D' = 1$ and $LOD \geq 2$; shades of pink/red to $D' < 1$ and $LOD \geq 2$, blue to $D' = 1$ and $LOD < 2$ and white $D' < 1$ and $LOD < 2$. **B**, Seven major *CYP2C8* haplotypes and the corresponding tSNPs were inferred with Haploview program using CEPH HapMap data. The HapMap frequency of the haplotypes is shown beside the nucleotide sequence. There are 6 HapMap-tSNPs which are marked with a triangle and correspond to: 1=rs7073968, 3=rs7077618, 6=rs11188148, 26=rs1341164, 99=rs1934956 and 105=rs17110453. Among the 12 SNPs that were genotyped and used for *CYP2C8* haplotype inference in the liver samples 8 are included in the picture and are marked with a black star. Specifically, 22=rs10509681, 35=rs2275620, 62=rs1113129, 83=rs2185571, 94=rs2275622, 99=rs1934956, 104=rs7909236 and 105=rs17110453. Arrows connect SNPs in total L.D. with the HapMap tSNPs and a dashed line connects SNPs 1 and 62 which can both single out haplotype C3. The differences in nucleotide sequence between haplotypes B and E and those between haplotypes C and D and the rest of haplotypes are boxed. The nucleotide sequence of the 7 *CYP2C8* haplotypes was aligned and a phylogenetic tree comparing the different haplotypes constructed. HapMap data: Rel#20/phaseII Jan06, on NCBI B35 assembly, dbSNP b125.

Supplementary Figure 2. Asian and African *CYP2C8* haplotypes and MAF of the SNPs from HapMap Project data.

A, Linkage disequilibrium plots were obtained using Haploview with HapMap JPT and HCB data and **B**, YRI data. **C**, HapMap minimum allele frequencies (MAF) of *CYP2C8* SNPs in different ethnic groups. The haplotypes that have been associated to each *CYP2C8* SNP in the Caucasian population are shown in the Table. CEPH (northern and western Europe ancestry), HCB (Han Chinese in Beijing, China), JPT (Japanese in Tokyo, Japan) and YRI (Yoruba in Ibadan, Nigeria).

Supplementary Figure 3. *CYP2C8* haplotype/ phenotype association studies in healthy volunteers using repaglinide as probe drug.

Individual AUC(0-∞) values of repaglinide in 68 healthy subjects with different genotypes after a single oral dose of 0.25 mg repaglinide are shown. Subjects were first stratified according to the *SLCO1B1* 521T>C SNP followed by evaluation of the impact of *CYP2C8* haplotypes **A**, *CYP2C8* haplotype D (*CYP2C8**3); **B**, *CYP2C8* haplotype B and **C**, *CYP2C8* haplotype C. Horizontal bars show mean values for each genotype group. Subjects homozygous for the *CYP2C8* haplotypes B, C and D are represented by open circles in the corresponding graphs. The groups were compared by a 2-tailed t-test.

Supplementary Table 1. Oligonucleotides used for RT-PCR analysis.

Target mRNA	FW Primer	Forward primer sequence 5' to 3'	RV Primer	Reverse primer sequence 5' to 3'
CYP2C8 a.s.^a+ c.s.^b	Ex2-FW	TATGGTCCTGTGTTACCGT	Ex3-RV	TCAACTCCTCCACAAGGCAGT
CYP2C8 a.s.	In2-FW	CTTCTCAGCAGAGCTTAGCCTATC	Ex4-RV	ATTGAATCTTTTCATCAGGGTGAG
CYP2C8 c.s.	Ex2/3-FW	TCAAAGAATTACTAAAGGACTTGGAAAT	Ex4-RV	ATTGAATCTTTTCATCAGGGTGAG
β-actin	β -actin-FW	CGTACCACTGGCATCGTGAT	β -actin-RV	GTGTTGGCGTACAGGTCTTTGCG

^a Alternatively spliced mRNA (a.s.).

^b Correctly spliced mRNA (c.s.).

Supplementary Table 2. Oligonucleotides used for *CYP2C8* genotyping.

SNP	Primer Orientation	Primer Sequence	Size (bp)
rs17110453 (<i>CYP2C8*1C</i>)	FW	TTTGAAAGGCTTTTGTATCAAGGG	555 BsmFI
	RV	CAGCTCTGTCTCCAGAGTGAAAA	
rs7909236 (<i>CYP2C8*1B</i>)	FW	TTTGAAAGGCTTTTGTATCAAGGG	555
	RV	CAGCTCTGTCTCCAGAGTGAAAA	355
	A.S. FW	CAGCACATTGGAAC	
	A.S. FW	CAGCACATTGGAAA	
	A.S. RV	CAGCTCTGTCTCCAGAGTGAAAA	
rs11572080 (<i>CYP2C8*3-R139K</i>)	FW	CTTCTCAGCAGAGCTTAGCCTATC	238 BseRI
	RV	TCAACTCCTCCACAAGGCAGT	
rs10509681 (<i>CYP2C8*3-K399R</i>)	FW	ATGAAATAGAGCGGCAAATGA	378
	RV	AGTGGCCAGGGTCAAAGATA	355
	A.S. FW	ATGAAATAGAGCGGCAAATGA	
	A.S. RV	GGATTAGGAAATTCTT	
	A.S. RV	GGATTAGGAAATTCTC	
rs1058930 (<i>CYP2C8*4</i>)	FW	TCTGCAATAATTTCCCTCTAC	258
	RV	ATCCTTAGTAAATTACAGAAGG	168
	A.S. FW	GTCTGCAATAATTTCCCTCT	
	A.S. RV	TTTTGATCAGGAAGCAATCG	
	A.S. RV	TTTTGATCAGGAAGCAATCC	
rs2275622 (<i>I2-64</i>)	FW	TATGGTCCTGTGTTACCCGT	460
	RV	TCAACTCCTCCACAAGGCAGT	209
	A.S. FW	TCTGCATGGCTGCCG	
	A.S. FW	TCTGCATGGCTGCCA	
	A.S. RV	CTCCACAAGGCAGTGA	
rs3216029 /rs11572078 (<i>I2-13</i>)	FW	TATGGTCCTGTGTTACCCGT	460
	RV	TCAACTCCTCCACAAGGCAGT	214
	A.S. FW	GGCAATCCCCAATA	
	A.S. RV	TTCCTAATAAAAAAAAAA	
	A.S. RV	TTCCTAATAAAAAAAAAAG	
rs1113129 (<i>I5-5324</i>)	FW	GCAGAAAATCTGGGCAATACA	442
	RV	GCAGAGATTGTGGAGCTGAA	366 AluI
	FW	GCAGAAAATCTGGGCAATACA	
	RV	GAATTGATTTCAGCAGAAGAAAGAATTAGTGTG	
rs11188172 (<i>Pr-2048</i>)	FW	AGAAACAAGGAGCAGAGCAA	
	RV	GCTAAGGACACACAGAATGCAA	
rs2275620 (<i>I7 +49</i>)	FW	GGAGCCACATGCCTTACACT	497
	RV	AAGCTCAATAAGTTGGGAGCA	189
	A.S. FW	GGAGCCACATGCCTTACACT	
	A.S. RV	AACCAAACCAGCACTA	
	A.S. RV	AACCAAACCAGCACTT	
rs1934956 (<i>I1-712</i>)	FW	CCTGGTGCTGTGTCTCTCTTT	1495 PfiMI
	RV	AATGACCCAGGCAATTGGTA	
rs2185571 (<i>I3-258</i>)	2C8-in3 FW	GGCTTTGCAAACAGACATGA	477
	2C8-in3 RV	ATTGAATCTTTTCATCAGGGTGAG	399
	A.S. FW	AATAAAAAGACACTTGGG	
	A.S. FW	AATAAAAAGACACTTGGAA	
	A.S. RV	ATTGAATCTTTTCATCAGGGTGAG	

Figure 1

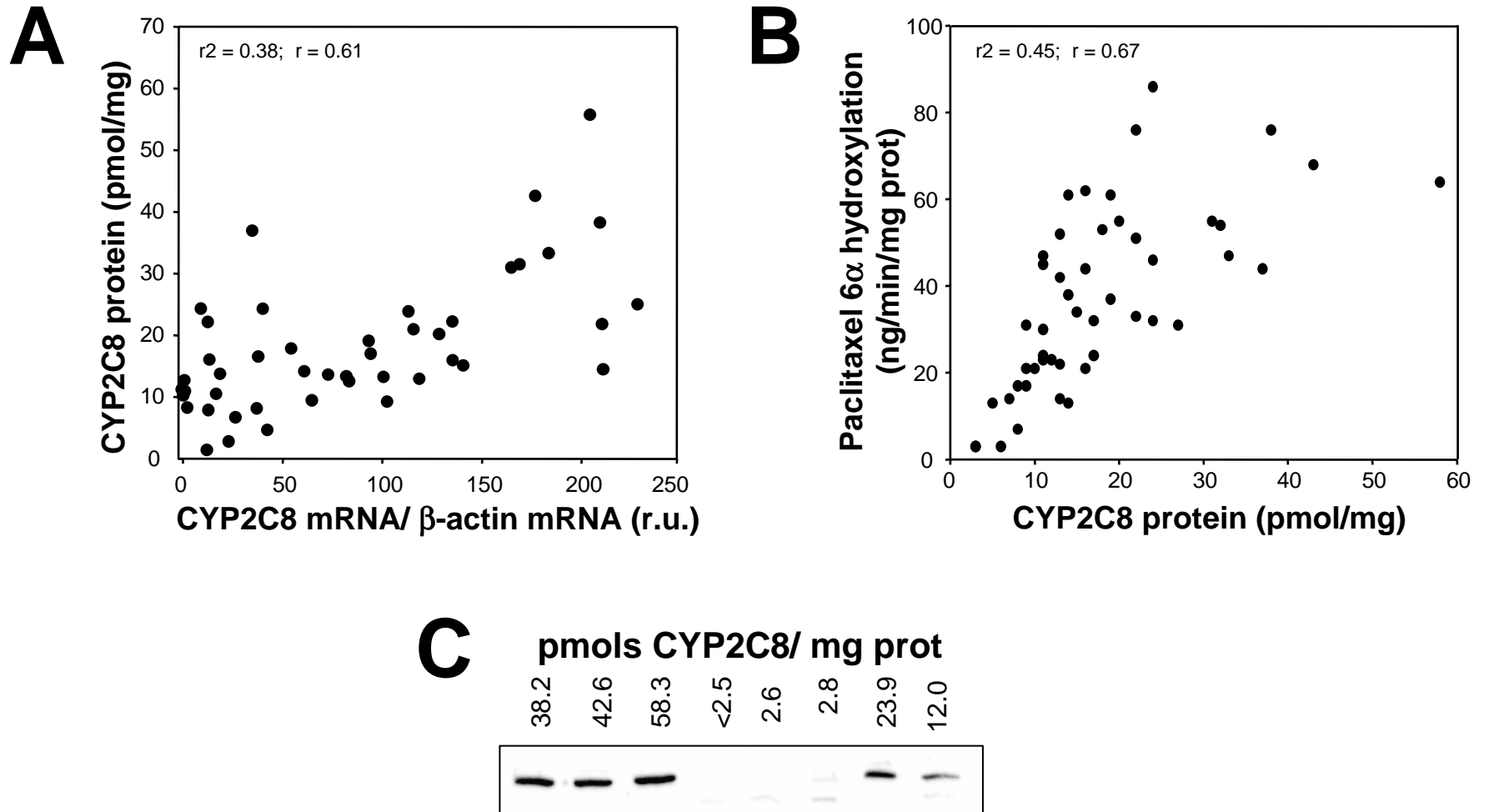


Figure 2

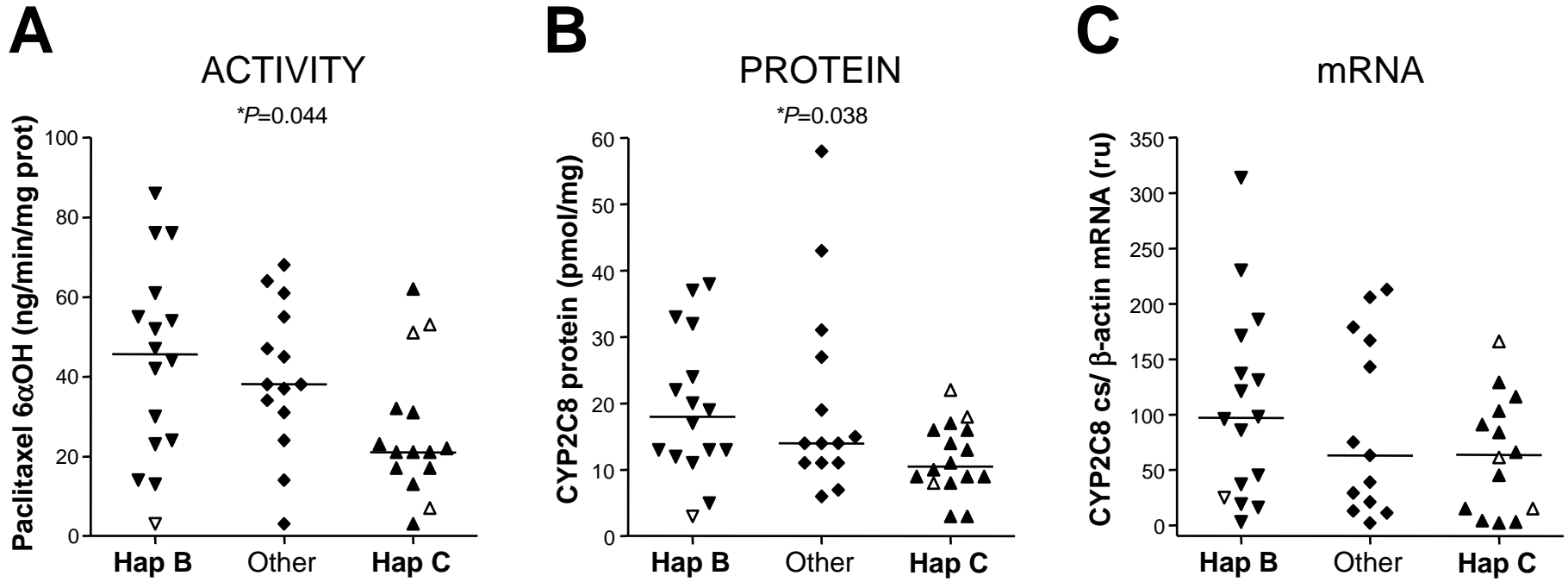
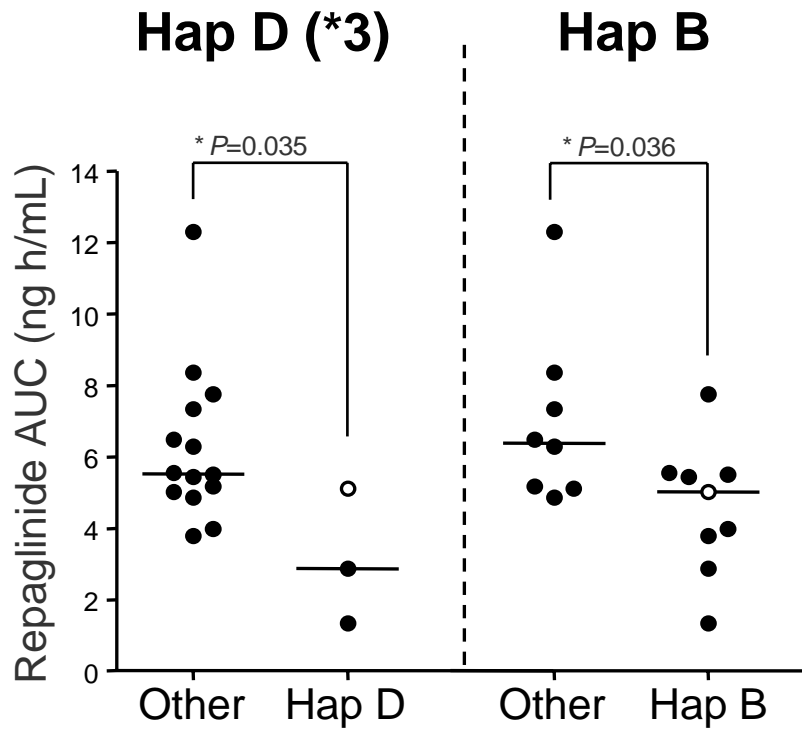


Figure 3

A

High activity



B

Low activity

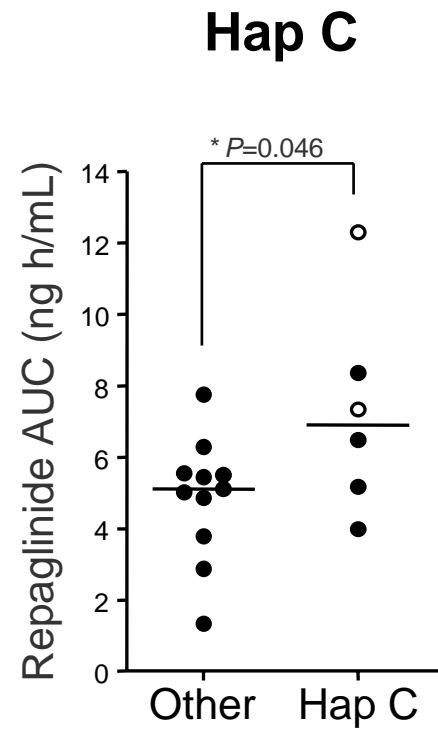


Figure 4

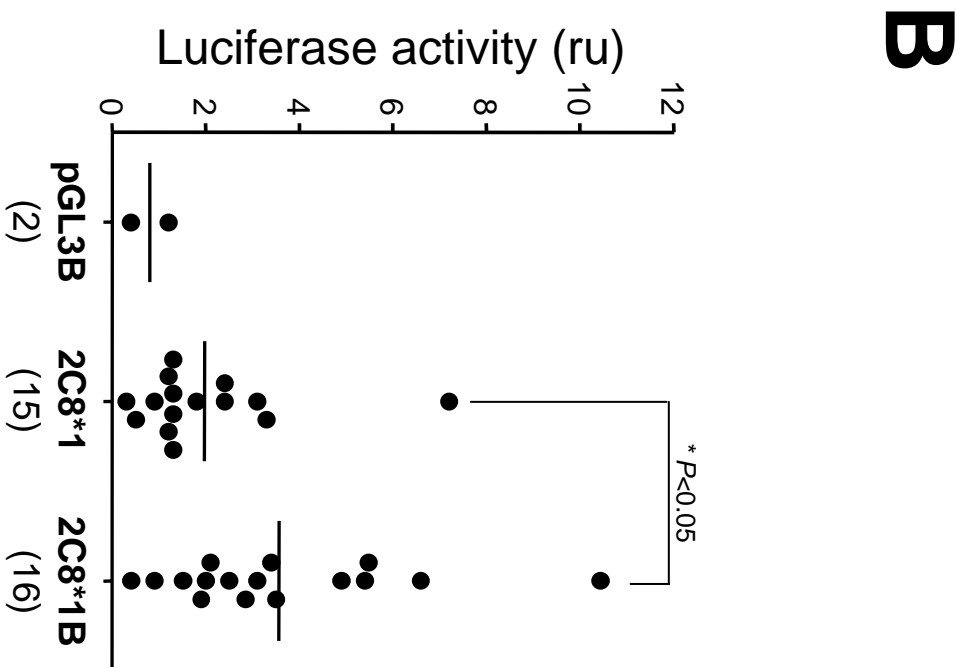
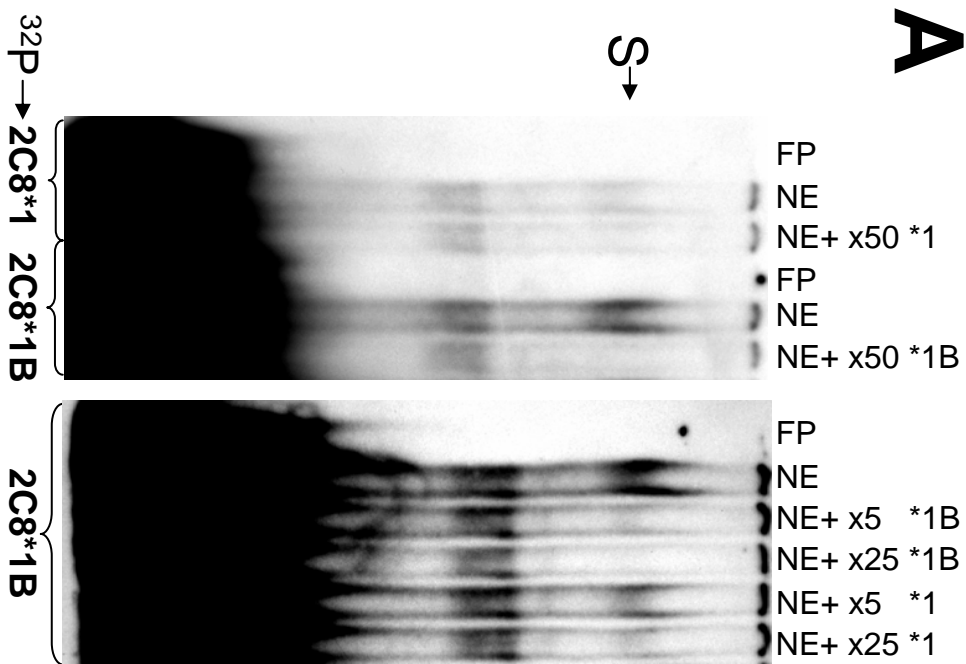
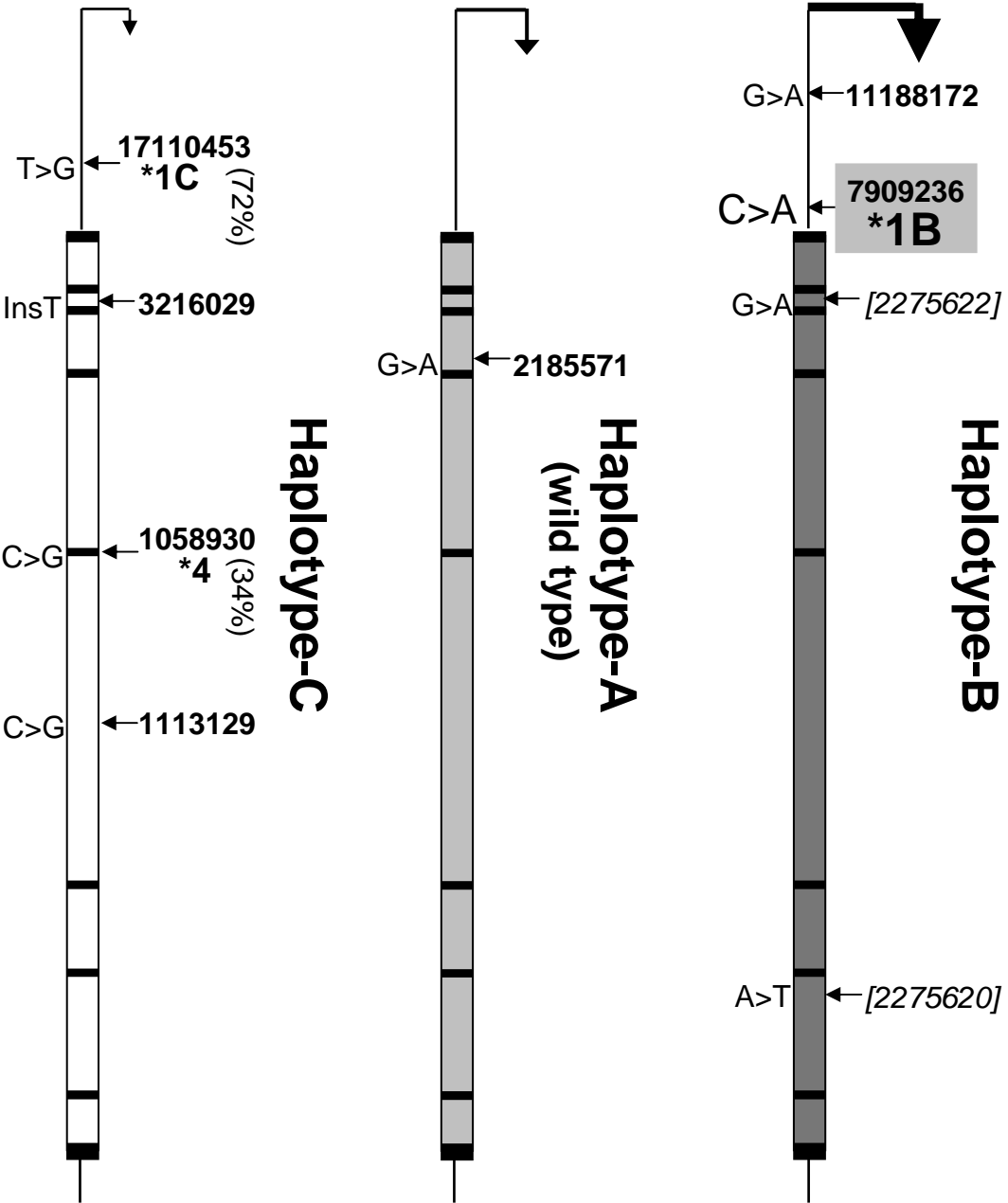


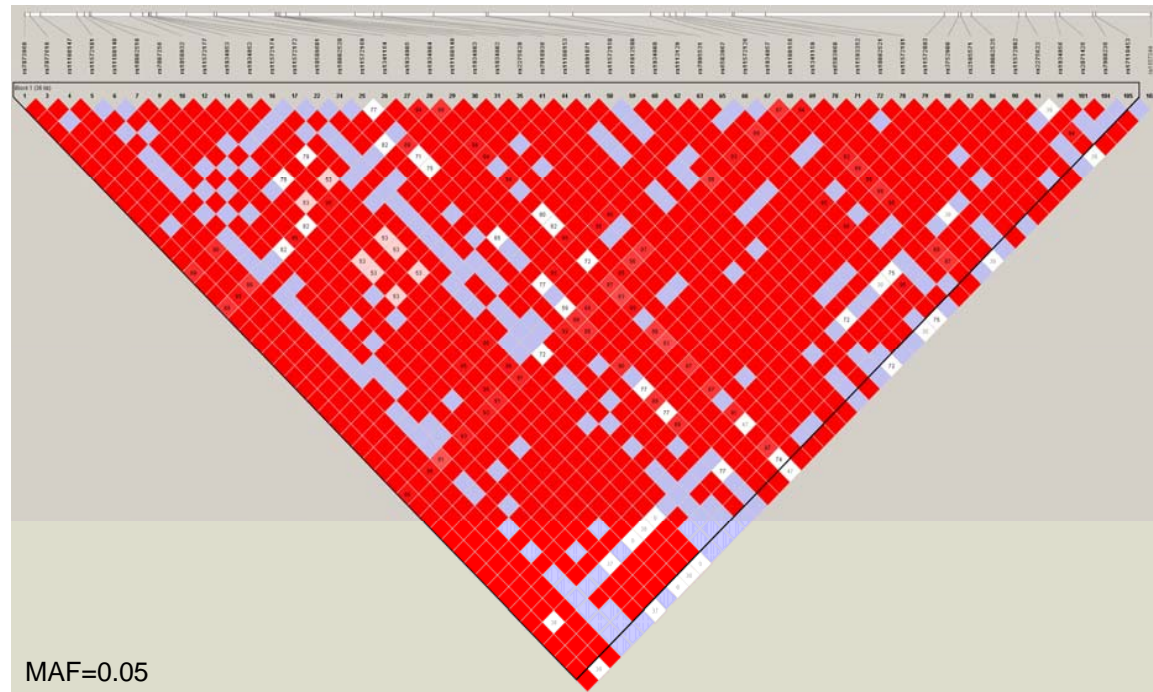
Figure 5



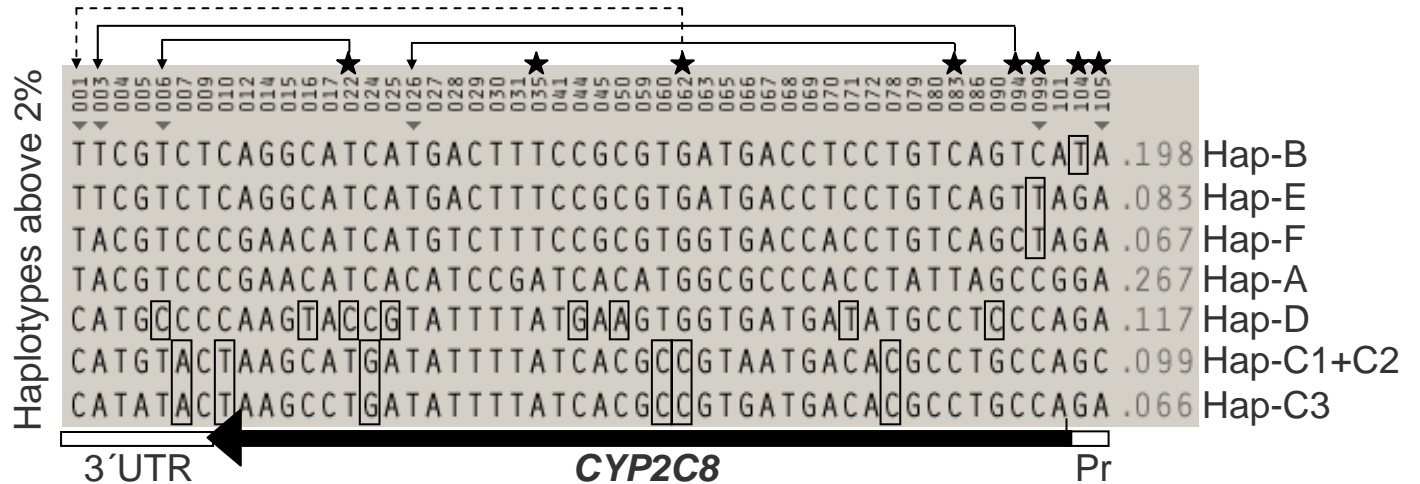
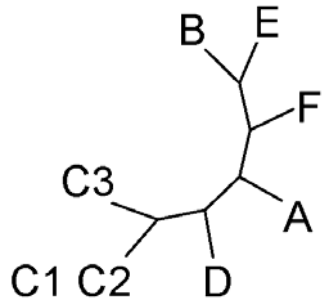
Supplementary Figure 1

A

CEPH: *CYP2C8* (40kb, chr10:96782845..96822844)

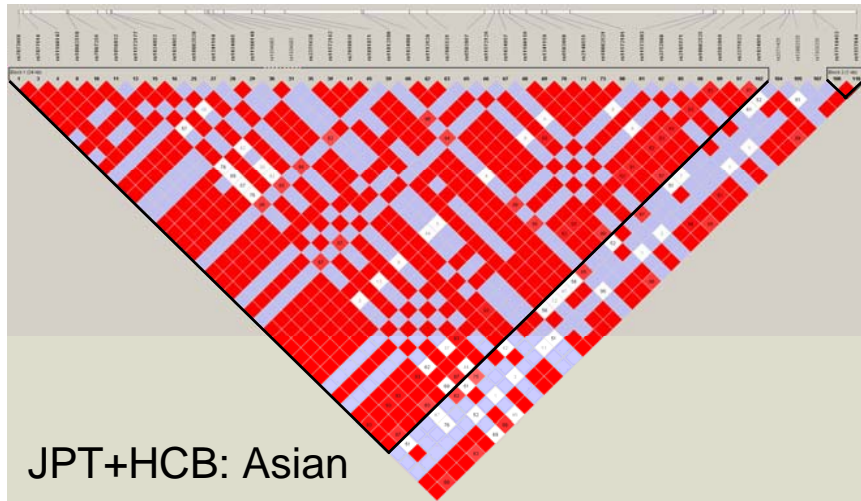


B

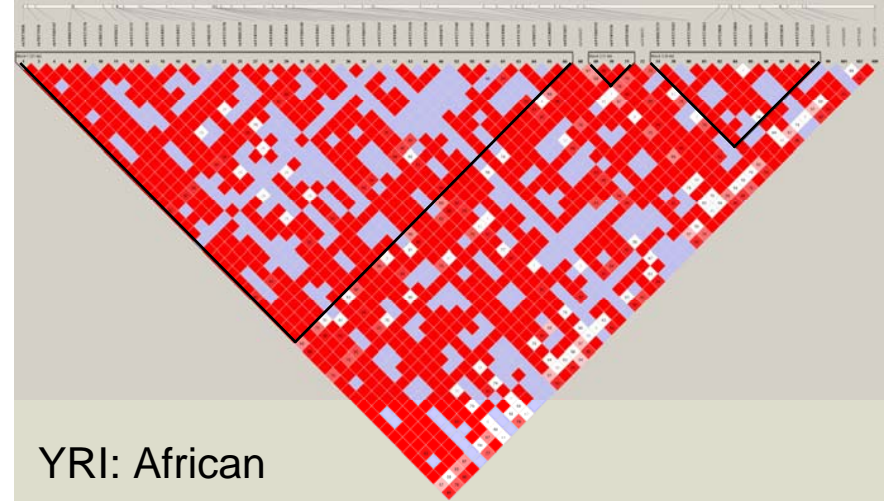


Supplementary Figure 2

A



B



C

RefSNP	2C8 Location	Haplotype	CEPH	HCB	JPT	YRI
rs17110453	Prom (*1C)	C1+C2	0.117	0.278	0.344	0.000
rs7909236	Prom (*1B)	B	0.233	0.100	0.089	0.000
rs1934956	intron 1	E	0.158	0.478	0.455	0.267
rs2185571	intron 3	A	0.300	0.056	0.057	0.100
rs1113129	intron 5	C	0.192	0.344	0.386	0.500
rs10509681	exon 8 (*3)	D	0.117	0.000	0.000	0.000

Supplementary Figure 3

